Pharm Res (2011) 28:1631–1642
DOI 10.1007/s11095-011-0398-5

RESEARCH PAPER

"Click" Conjugation of Peptide on the Surface of Polymeric Nanoparticles for Targeting Tumor Angiogenesis

Stéphanie Deshayes • Victor Maurizot • Marie-Claude Clochard • Cécile Baudin • Thomas Berthelot • Stéphane Esnouf • Didier Lairez • Michel Moenner • Gérard Déléris

Received: 1 December 2010 / Accepted: 8 February 2011 / Published online: 4 March 2011

ABSTRACT

Purpose Angiogenesis plays a critical role in tumor growth. This phenomena is regulated by numerous mediators such as vascular endothelial growth factor (VEGF). CBO-P11, a cyclo-peptide, has proven to specifically bind to receptors of VEGF and may be used as targeting ligand for tumor angiogenesis. We herein report the design of novel nanoparticles conjugated to CBO-P11 in order to specifically target tumor site.

Methods The conjugation of CBO-P11 on the surface of poly (vinylidene fluoride) (PVDF) nanoparticles was investigated using the copper(I)-catalyzed Huisgen 1,3-dipolar cycloaddition known as "click" reaction. CBO-P11 was modified with a near-infrared cyanine dye bearing an alkyne function, allowing both "click" coupling on azido-modified nanoparticles and fluorescence labelling. Each step of this nanodevice construction was judiciously performed in aqueous solution and successfully characterized. The cytotoxicity of nanoparticles was evaluated in human brain endothelial cell line and their affinity for VEGF receptors was determined *via* fluorescence-based uptake assays on porcine aortic endothelial cell line.

Results Nanoparticles were found to be spherical, dense, monodisperse and stable. No cytotoxicity was observed after four days of incubation, demonstrating the biocompatibility of nanoparticles. Fluorescence highlighted the specific interaction of these functionalized nanoparticles for VEGF receptors, suggesting that the targeting peptide bioactivity was retained.

Conclusions These results demonstrate the potential of these functionalized nanoparticles for targeting tumor angiogenesis and their possible use as multifunctional plateform for cancer treament if coupled with therapeutic agents.

KEY WORDS angiogenesis · "click" chemistry · cyclo-peptide · nanoparticles · PVDF · tumor targeting

ABBREVIATIONS

AA	acrylic acid
ACN	acetonitrile
DCM	dichloromethane
DIEA	diisopropylethylamine
DLS	dynamic light scattering
DMEM	Dulbecco's modified eagle medium
EDC	ethyl-3(3dimethylaminopropyl)carbodiimide
EDTA	ethylenediaminetetraacetic acid
EGM-2	endothelial growth medium
ESI	electrospray ionization
FBS	fetal bovine serum

Electronic supplementary material The online version of this article (doi:10.1007/s11095-011-0398-5) contains supplementary material, which is available to authorized users.

S. Deshayes · V. Maurizot · G. Déléris
CNAB, Chimie Bio-Organique UMR CNRS 5084
Université de Bordeaux 2
33076 Bordeaux, France

S. Deshayes · M.-C. Clochard (✉) · C. Baudin · T. Berthelot
Laboratoire des Solides Irradiés UMR CNRS-CEA 7642
Ecole Polytechnique
28 route de Saclay
91128 Palaiseau, France
e-mail: marie-claude.clochard@polytechnique.edu

S. Esnouf
Laboratoire de Radiolyse, Service de Chimie Moléculaire
UMR CNRS-CEA 3299
91191 Gif-Sur-Yvette, France

D. Lairez
Laboratoire Léon Brillouin UMR CNRS-CEA 12
91191 Gif-Sur-Yvette, France

M. Moenner
Laboratoire des Mécanismes Moléculaires de l'Angiogenèse
INSERM U920 Université de Bordeaux 1
33405 Talence, France

FESEM	field emission scanning electron microscope
FTIR	fourier transform infrared
HCMEC	human brain endothelial cells
HOBt	*N*-hydroxybenzotriazole
HPLC	high-performance liquid chromatography
HUVEC	human umbilical vein endothelial cells
IC_{50}	half-maximal inhibitory concentration
Ip	polydispersity index
MALDI-TOF	matrix-assisted laser desorption/ionization-time of flight
mTEG	modified tetraethyleneglycol
NIR	near-infrared
NMP	*N*-methylpyrrolidone
NMR	nuclear magnetic resonance
PAA	poly(acrylic acid)
PAE	porcine aortic endothelial cells
PBS	phosphate-buffered saline
POA	perfluorooctanoic acid
PVDF	poly(vinylidene fluoride)
Rg	radius of gyration
Rh	hydrodynamic radius
SANS	small-angle neutron scattering
SLS	static light scattering
t-BuOH	*tertio*-butanol
TFA	trifluoroactic acid
THF	tetrahydrofurane
TIS	triisopropylsilane
UV	ultra-violet
VEGF	vascular endothelial growth factor
VEGFR	receptor of VEGF
VF2	vinylidene fluoride
WST-1	4-[3-(4-iodophenyl)-2-(4-nitrophenyl)-2H-5-tetrazolio]-1,3-benzene disulfonate
XPS	X-ray photoelectron spectroscopy

INTRODUCTION

Lack of selectivity in cancer therapies is one of the major limitations of chemotherapies due to their strong side effects. The quest for tumor-specific treatments has led to the development of nanoparticulate drug delivery systems (1). Indeed, polymeric nanoparticles gained considerable attention in recent years because they offer two strategic pathways: passive and active targeting. Passive targeting occurs by passive accumulation of polymeric nanoparticles preferentially in tumor tissues by enhanced permeation and retention effects of malignant vessels compared to healthy vessels (2). On the other hand, nanoparticles which have a high surface area can carry a large number of biological molecules such as ligands that specifically bind to overexpressed receptors in the tumor region; this is named active targeting. Among targeting agents, anti-angiogenic peptides have received intense interest (3). Angiogenesis is the development of new blood vessels from existing ones and plays a critical role in controlling tumor growth and metastasis. Indeed, Folkman hypothesized in 1971 that tumor growth requires the elaboration of vascular network to supply nutrients and oxygen avoiding hypoxia and tumor cell apoptosis (4). Angiogenesis is regulated by a balance of positive and negative mediators. Among them, vascular endothelial growth factor (VEGF) is a key factor in tumor growth; it regulates endothelial cell proliferation, permeability, and survival. VEGF exerts its action *via* binding to two main receptor-type tyrosine kinase: VEGFR-1 (known also as Flt-1) and VEGFR-2 (known also as KDR) (5–7). These receptors are overexpressed on tumor-associated endothelial cells (8–10). Thus, blocking tumor angiogenesis appears to be an attractive target to inhibit specifically tumor growth without damaging normal cells. In our laboratory, we have synthesized a 17-amino acid molecule designated cyclo-peptidic vascular endothelial growth inhibitor (cyclo-VEGI or CBO-P11) encompassing residues 79–93 of VEGF which are involved in the interaction with VEGFR-2 (11). CBO-P11 shows a micromolar affinity for VEGFR-2 and can be used as a tumor targeting agent.

In this paper, we present an elegant strategy for the conjugation of this peptidic ligand on poly(vinylidene fluoride) (PVDF) nanoparticles which could be used as a novel tool for targeting tumor angiogenesis. PVDF was chosen due to its known non-toxicity, biocompatibility, and chemical stability properties (12). Commercially available PVDF devices are in use for medical application. For example, XIENCE V™ utilizes the MULTI-LINK VISION® stent, the antiproliferative drug everolimus, a fluorinated polymer drug carrier, poly(vinylidene fluoride-co-hexafluoropropylene) (PVDF-HFP) and a stent-specific delivery system (13). PVDF is also used for surgical mesh (DynaMesh® for abdominal hernia repair) (14–16). Other applications have been as well reported, such as membranes for osteoblast adhesion (17) or nerve regeneration (18). Although PVDF has been used for biomedical applications, literature lacks reports about the use of PVDF nanoparicles as nanocarrier. PVDF is a hydorphobic polymer, suggesting that it could be coated with a hydrophilic layer to get a core/shell structure and then can be used as drug delivery system. According to an optimized process from a preliminary study (19), nanoparticles were consequently coated with poly(acrylic acid) (PAA), using electron-beam irradiation yielding PVDF-g-PAA nanoparticles.

To achieve the conjugation of CBO-P11 to PVDF-g-PAA nanoparticles without modifying the bioactivity of targeting peptide, we investigated "click" reaction, which has received much attention for preparation of bioconjugated systems due to its high degree of selectivity and stability and its potential use under physiological aqueous

conditions (20–22). We have chosen to take advantage of Huisgen 1,3-dipolar cyclo-addition to conjugate alkyne-peptide and azido polymeric nanoparticles (Scheme 1). First, CBO-P11 was coupled with a fluorescent cyanine dye bearing an alkyne function (Scheme 2). Subsequently, carboxylic functions on the surface of PVDF-g-PAA nanoparticles were coupled with an amine-terminated azido spacer arm derived from oligoethylene glycol. This ethylene glycol chain aims to increase the hydrophilicity of nanoparticles and space the future biologically active molecule away from the core of the nanoparticles.

A detailed characterization was performed to assess the morphology of nanoparticles and the grafting location. Furthermore, *in vitro* cytotoxicity and uptake studies were performed on endothelial cells in order to check the biocompatibility of these nanoparticles and the keeping of the peptide affinity for VEGF receptors.

MATERIALS AND METHODS

Materials

The following chemicals were purchased from Sigma-Aldrich (Saint-Quentin Fallavier, France) and used as received: paraffin Wax, potassium persulfate, perfluorooctanoic acid (POA), acrylic acid (AA) stabilized with 200 ppm hydroquinone, propargylamine, piperidine, diisopropylethylamine (DIEA), copper sulfate, sodium ascorbate, trifluoroactic acid (TFA), triisopropylsilane (TIS) and 4-carboxy TEMPO. Vinylidene fluoride (VF2) monomer was provided by Solexis (Yverdon-les-Bains, Switzerland). *N*-hydroxybenzotriazole (HOBt), Ethyl-3(3dimethylaminopropyl)carbodiimide (EDC), phenol and potassium bromide were obtained from Fluka (Saint-Quentin Fallavier, France). The HPLC grade solvents dichloromethane (DCM), tetrahydrofurane (THF) and acetonitrile (ACN) were provided from VWR (Fontenay sous Bois, France). *N*-methylpyrrolidone (NMP) was purchased from Applied Biosystems (Villebon-sur-Yvette, France). *Tertio*-butanol (*t*-BuOH) was purchased from Acros Organics (Geel, Belgium). Fmoc-Lys(Boc)-OH was provided by Novabiochem (Darmstadt, Germany). Thioanisole and ethylenediaminetetraacetic acid (EDTA) were purchased from Alfa Aesar. Endothelial growth medium (EGM-2) Bulletkit was purchased from Cambrex (Walkersville, USA). Human brain endothelial cells (HCMEC) were kindly provided by P.O. Couraud (Institut Cochin, Paris, France) and were grown as previously reported by Weksler *et al.* (23). Porcine aortic endothelial cells stably transfected with VEGFR-2 (PAE) were a gift from Dr. Lena Claesson-Welsh (Ludwig Institute, Uppsala, Sweden). Dulbecco's modified eagle medium (DMEM) was purchased from Invitrogen (Cergy Pontoise, France). 4-[3-(4-iodophenyl)-2-(4-nitrophenyl)-2H-5-tetrazolio]-1,3-benzene disulfonate (WST-1) was provided from Roche Applied Science (Indianapolis, IN, USA).

Synthesis of PVDF Nanoparticles

PVDF nanoparticles were prepared by emulsion polymerization of corresponding monomer (VF2) as previously described (19). Two different syntheses were run in the presence or in the absence of surfactant. Briefly, 3 l of an aqueous solution consisting of paraffin (40 g, 10% in weight of monomer), potassium persulfate initiator (400 mg, 1.5 mmol) and, only for the second synthesis, perfluorooctanoic acid surfactant (10 g, 24 mmol) and potassium hydroxide (1.5 g, 27 mmol) were put in a stirred autoclave under vacuum. The mixture was then heated to 40°C and stirred at 800 rpm. The reactor was fed with VF2 gaseous monomer (400 g, 6.2 mol) to reach desired pressure (100 bars) while the temperature carried on rising up to 80°C.

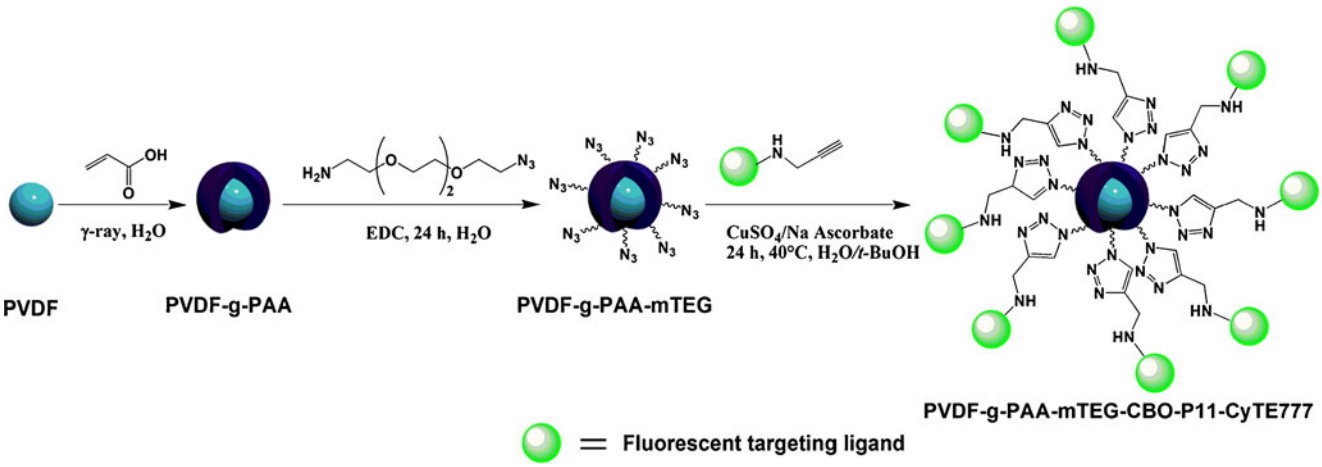

Scheme 1 Functionalization of PVDF nanoparticles. Radio-grafting of PAA, coupling with azido spacer arm (mTEG) and "click" conjugation of fluorescent targeting ligand (CBO-P11-CyTE777).

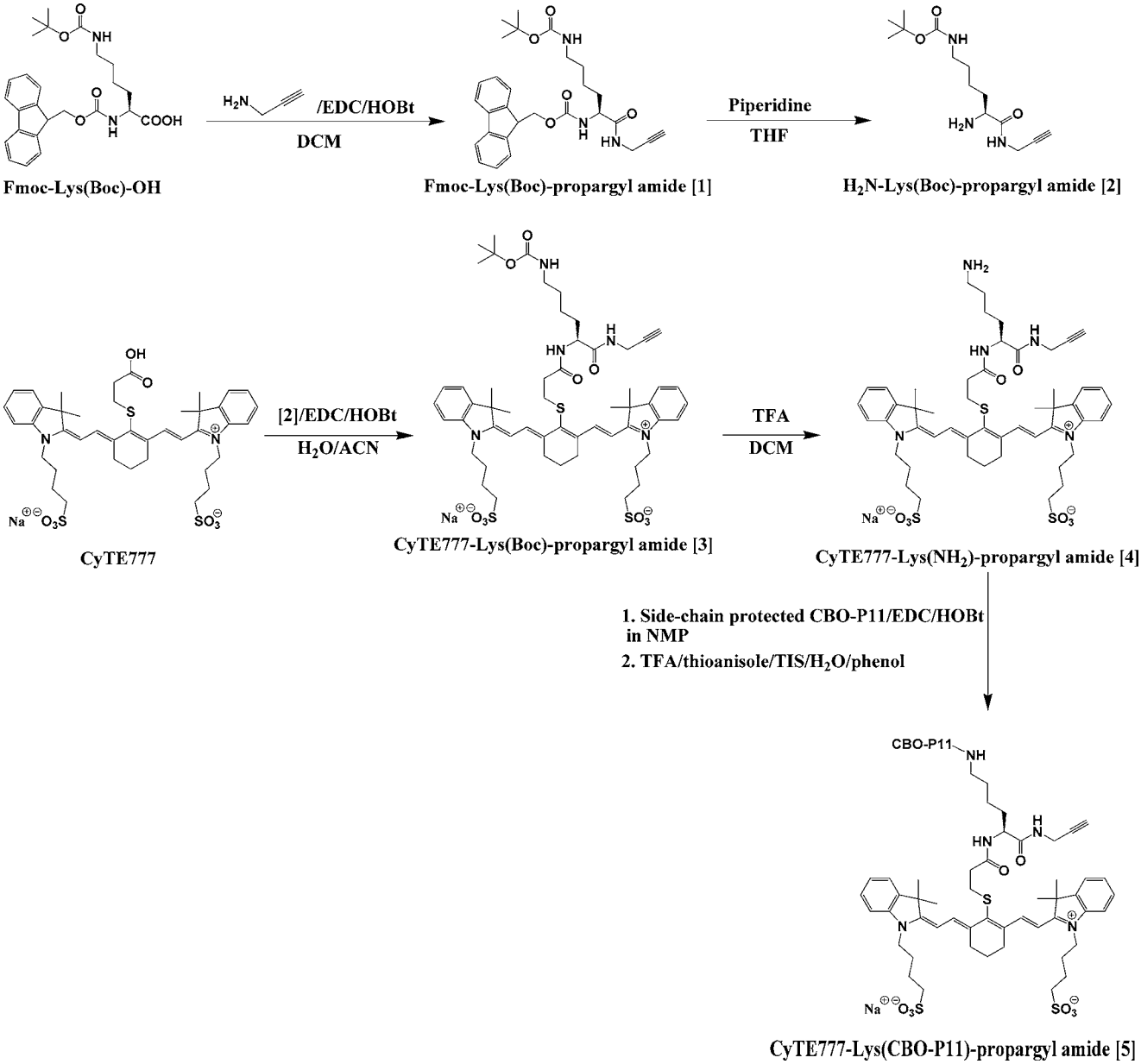

Scheme 2 Synthesis of fluorescent targeting ligand CyTE777-Lys(CBO-P11)-propargyl amide.

When pressure decreased under 80 bars for the first synthesis and 60 bars for the second one, stirring was stopped. After the removal of the supernatant containing paraffin, the latex dispersion made of PVDF nanoparticles in suspension was used without further purification.

In Situ Radiation Grafting of PVDF with Acrylic Acid

PAA grafting onto PVDF nanoparticles was directly achieved upon γ-irradiation of PVDF nanoparticles dispersed (10 mg/ml) in a 2% AA aqueous solution. The irradiation was performed at room temperature under vacuum, using a Gammacell 3000 Elan, MDS Nordion irradiator from a ^{137}Cs source in the 1–10 kGy dose range at 0.33 kGy/h dose rate. Then, the mixture was washed with distilled water by filtration on 0.05μm Millipore membranes to completely remove the homopolymer and the unreacted monomer.

Covalent Coupling of Spacer Arm

The spacer arm noted mTEG was synthesized as described in a previous paper (24). mTEG (10 eq.) was coupled to PVDF-g-PAA nanoparticles (5 mg/ml) *via* an amide bond to the carboxylic acid functions of PAA using EDC (10 eq.) at room temperature for 24 h under mechanical stirring.

Then, the dispersion was purified by dialysis using Spectra/Por membrane (MW: 50,000 Da) for 3 days. The PVDF-g-PAA-mTEG nanoparticles were kept in water to avoid aggregation.

Synthesis of Fmoc-Lys(Boc)-propargyl Amide [1]

To a solution of Fmoc-Lys(Boc)-OH (3.74 g, 8 mmol) in DCM (60 ml), EDC (1.7 ml, 9.6 mmol) and HOBt (1.47 g, 9.6 mmol) were added. The mixture was stirred at room temperature for 30 min. Then, propargylamine (1.1 ml, 16 mmol) was added, and the resulting solution was stirred for 12 h. The crude product dissolved in DCM was washed with 10 ml of 1 M HCl solution. A white precipitate was formed and removed by filtration. The organic phase was washed with water and dried over $MgSO_4$, and solvent was evaporated under reduced pressure. The solid was rinsed with diethyl ether and dried to give a pale yellow solid (3.56 g, 88%) without further purification. The product was analyzed by reversed-phase HPLC with the following gradient: 30% of eluant B for 5 min and 30%–100% for 10 min; detector: 214 nm, tr = 21.8 min and purity = 95%. ^{1}H NMR (300 MHz, $CDCl_3$): δ = 1.34–1.55 (m, 4 H, $CH_2CH_2CH_2CH_2$), 1.45 (s, 9 H, $(CH_3)_3C$), 1.69 (q, 1 H, J = 7.6 Hz, $CHCH_2CH_2$), 1.86 (q, 1 H, J = 7.6 Hz, $CHCH_2CH_2$), 2.16 (br s, 1 H, $CH_2C{\equiv}CH$), 3.11 (br s, 2 H, CH_2CH_2NH), 4.03 (br s, 2 H, $NHCH_2C{\equiv}CH$), 4.23 (t, 2 H, J = 5.9 Hz, $CHCH_2$ and $NHCHCO$), 4.41 (d, 2 H, J = 5.5 Hz, $CHCH_2CO$), 4.73 (br s, 1 H, NHBoc), 5.74 (d, 1 H, J = 6.4 Hz, NHFmoc), 6.83 (br s, 1 H, $CONHCH_2$), 7.31 (t, 2 H, J = 7.3 Hz, CH_{Ar}), 7.41 (t, 2 H, J = 7.0 Hz, CH_{Ar}), 7.59 (t, 2 H, J = 6.7 Hz, CH_{Ar}) and 7.77 (t, 2 H, J = 7.1 Hz, CH_{Ar}). ^{13}C NMR (75.5 MHz, $CDCl_3$): δ = 22.5 ($CH_2CH_2CH_2$), 28.5 ($(CH_3)_3C$), 29.2 ($CH_2CH_2CH_2$), 29.6 ($NHCH_2C{\equiv}CH$), 32.01 ($CHCH_2CH_2$), 47.2 (CH_2CH_2NH), 53.5 ($CHCH_2$), 54.7 ($NHCHCO$), 67.2 ($CHCH_2CO$), 71.9 ($CH_2C{\equiv}CH$), 75.5 ($CH_2C{\equiv}CH$), 79.2 ($(CH_3)_3C$), 120.1 (2 CH_{Ar}), 125.2 (2 CH_{Ar}), 127.1 (2 CH_{Ar}), 127.8 (2 CH_{Ar}), 141.4 (2 C_{Ar}), 143.8 (2 C_{Ar}), 156.5 ($COBoc$ and $COFmoc$) and 171.7 ($NHCO$). Mass analysis (MALDI-TOF): m/z 528.1900 (calcd for $C_{29}H_{35}N_3O_5Na$ [M^+] m/z 528.5951).

Synthesis of H_2N-Lys(Boc)-propargyl Amide [2]

Fmoc-Lys(Boc)-propargyl amide (450 mg, 0.89 mmol) was dissolved in 3% piperidine in THF (30 ml). After the mixture was stirred for 5 h at room temperature, solvent was removed under reduced pressure, and the residue was coevaporated three times with toluene. Petroleum ether (10 ml) was added to the crude product, and the supernatant containing the dibenzofulvene-piperidine adduct was removed. The residue was dried under vacuum and was used as is without further purification. Mass analysis (ESI): m/z 284.1968 (calcd for $C_{14}H_{26}N_3O_3$ [M^+] m/z 284.3666).

Synthesis of CyTE777-Lys(Boc)-propargyl Amide [3]

The CyTE777 NIR dye was synthesized as previously reported by Hilderbrand *et al.* (25). To a solution of CyTE777 (180 mg, 0.22 mmol) in a mixture H_2O/ACN (1/1) (30 ml), EDC (47 μl, 0.26 mmol) and HOBt (40 mg, 0.26 mmol) were added. The mixture was stirred at room temperature for 30 min. Then, H_2N-Lys(Boc)-propargyl amide (156 mg, 550 μmol) was added, and the resulting solution was stirred for 5 h. The solvent was removed under reduced pressure, and the residue was used as is without further purification. Mass analysis (ESI): m/z 1084.4526 (calcd for $C_{55}H_{75}N_5O_{10}S_3Na$ [M^+] m/z 1084.4568).

Synthesis of CyTE777-Lys(NH_2)-propargyl Amide [4]

CyTE777-Lys(Boc)-propargyl amide (174 mg, 0.16 mmol) was dissolved in a mixture of DCM/TFA (1/1) (6 ml). After the mixture was stirred for 2 h 30 at room temperature, DCM was evaporated under reduced pression. Then, water was added, and the mixture was freeze-dried. The product was purified by preparative HPLC with the following gradient: 0% B for 5 min, increase up to 20% B in 5 min, 20% B for 10 min, increase up to 100% B in 10 min and 100% B for 10 min, λ_{max} of detector: 740 nm, tr = 33.5 min. ACN was evaporated and the aqueous solution was freeze-dried to give a green solid (83 mg, 53%). UV-visible (H_2O): λ_{max} = 782 nm (49,000 $M^{-1}cm^{-1}$). ^{1}H NMR (300 MHz, CD_3OD): δ = 1.28–1.49 (m, 2 H), 1.56–1.71 (m, 4 H), 1.77 (s, 12 H), 1.86–2.12 (m, 10 H), 2.53 (t, 1 H, J = 2.6 Hz), 2.55–2.63 (m, 2 H), 2.65–2.80 (m, 2 H), 2.89 (tt, 8 H, J = 7.2 Hz), 3.08 (t, 2 H, J = 7.0 Hz), 3.91 (t, 2 H, J = 2.7 Hz), 4.23 (t, 4 H, J = 7.3 Hz), 4.88–4.93 (m, 1 H), 6.35 (br s, 2 H), 7.19–7.56 (m, 8 H), 8.90 (br s, 2 H). Mass analysis (ESI): m/z 984.4044 (calcd for $C_{50}H_{67}N_5O_8S_3Na$ [M^+] m/z 984.4088).

Synthesis of CyTE777-Lys(CBO-P11)-propargyl Amide [5]

CBO-P11, cyclo(*D*FPQIMRIKPHQGQHIGE) peptide with protected side chains was synthesized by Fmoc/*t*-butyl batch solid phase synthesis on an Applied Biosystems 433A automated peptide synthesizer as previously described by Zilberberg *et al.* (11). To a solution of side-chain protected CBO-P11 (371 mg, 0.10 mmol) in NMP (4 ml), EDC (47 μl, 0.26 mmol), HOBt (42 mg, 0.26 mmol) and DIEA (66 μl, 0.39 mmol) were added. The mixture was stirred at room temperature for 30 min. Then, CyTE777-Lys(NH_2)-propargyl amide (78 mg, 80 μmol) was added, and the

resulting solution was stirred for 24 h. After addition of water (20 ml), a precipitate was formed, removed by filtration and dried under vacuum. Then, side-chain peptide protections were removed with a solution of TFA/phenol/water/thioanisole/TIS (10/0.75/0.5/0.5/0.25 v/w/v/v/v). Ten ml of this solution were added to 368 mg of product. The mixture was stirred for 3 h at room temperature. After addition of diethyl ether (30 ml), a white precipitate was formed, removed by filtration and dried under vacuum to give a green solid (283 mg, 92%). The product was analyzed by reversed-phase HPLC with the following gradient: 30% of eluant B for 5 min, 30%–50% for 5 min, 50% for 10 min, 50%–100% for 5 min and 100% for 5 min; detector: 785 nm, tr = 26.5 min and purity = 90%. UV-visible (H_2O): $\lambda_{max} = 787$ nm (56,000 $M^{-1}cm^{-1}$). Mass analysis (MALDI-TOF): *m/z* 2943.10 (calcd for $C_{140}H_{205}N_{33}O_{29}S_4$ [M^+] *m/z* 2942.58).

Conjugation of CyTE777-Lys(CBO-P11)-propargyl Amide to Azido-nanoparticles by "Click" Chemistry

An excess of [5] (2 eq.) was added to a solution of PVDF-g-PAA-mTEG (nanoparticles irradiated at 5 kGy) using copper sulfate (0.5 mM) and sodium ascorbate (1 mM) at 40°C for 24 h in a mixture of H_2O/*t*-BuOH (1/1) (16 ml). Nanoparticles were washed with a 1 mM EDTA solution in order to remove copper catalyst by filtration on 0.05 μm Millipore membranes. Then, nanoparticles were dialyzed using Spectra/Por membrane (MW: 50,000 Da) for 3 days against water to obtain a 1.4 mg/ml PVDF-g-PAA-mTEG-CBO-P11-CyTE777 nanoparticles aqueous suspension. In order to obtain a control sample without targeting peptide, PVDF-g-PAA-mTEG-CyTE777 nanoparticles were synthesized in a similar way using the fluorescent dye [4].

Cytotoxicty Assays

HCMEC were grown on a 0.2% gelatine matrix in EGM-2 at 37°C, 5% CO_2 up to confluence. After trypsinization, cells were washed with DMEM containing 10% FBS by centrifugation (800 rpm for 5 min). One hundred microliters of the cell suspension containing 7.5×10^3 cells were inoculated into each well of 96-well plates, and cells were allowed to settle for one night. Nanoparticles (PVDF, PVDF-g-PAA, PVDF-g-PAA-mTEG and PVDF-g-PAA-mTEG-CBO-P11-CyTE777) were then added at different concentrations (0, 0.1, 0.3, 1.1, 3.3, 11, 33 and 100 μg/ml) to each well. After 2, 3 or 4 days incubation with nanoparticles (except for PVDF-g-PAA-mTEG-CBO-P11-CyTE777, incubation for only 3 days), 5 μl of WST-1 was added to cell medium, and absorbance was determined after 2 h at 440 nm using an ELISA microplate reader (Molecular Devices Corporation). Results were analyzed using the Softmax Pro 4.0 software (Molecular Devices Corporation). The assay was performed in triplicates. Cells were counted using a cell counter (Coulter, Becton Dickinson).

Cell Uptake Assays

Cell uptake experiments were performed using a porcine aortic endothelial (PAE) cell line modified to overexpress VEGFR-2. PAE cells were inoculated into 96-well plates and grown up to confluency on a 0.2% gelatine matrix in EGM-2 at 37°C, 5% CO_2. They were then washed with DMEM and incubated for 45 min at 37°C in the same basal medium. Cells were then cultured in incomplete EGM-2 medium in the presence or absence of 100 ng/ml VEGF for 45 min at 37°C. Nanoparticles (PVDF-g-PAA-mTEG-CyTE777 and PVDF-g-PAA-mTEG-CBO-P11-CyTE777) were added at different fluorophore concentrations (1.4 μM; 466 nM; 155 nM; 52 nM; 17.3 nM; 5.8 nM; 1.9 nM; 640 pM). After a 12-h incubation at 37°C in the presence of nanoparticles, PAE cells were washed three times with PBS, and 96-well plates were analyzed using the Odyssey scanner.

RESULTS AND DISCUSSION

Synthesis and Characterization of PVDF Nanoparticles

Radical polymerization in aqueous emulsion was used to produce PVDF nanoparticles according to a previously described procedure (19). In order to assess the influence of surfactant on the size of these particles, two different batches of PVDF nanoparticles were prepared in the presence or in the absence of perfluorooctanoic acid (POA). Perfluorinated surfactants present a better active surface due to their high acid strength compared to hydrocarbon surfactants and promote micellization at lower concentration (26). The size, morphology and stability of nanoparticles were determined by field emission scanning electron microscopy (FESEM), static light scattering (SLS), dynamic light scattering (DLS) and small-angle neutron scattering (SANS). Table I summarizes data observed by these different techniques. In the absence of POA, the particles were two-fold larger than in the presence of POA. Surfactant stabilized the emulsion and contributed to minimize the size of the nanoparticles. The ratio between the radius of gyration and the hydrodynamic radius (R_g/R_h), which is a characteristic of nanoparticles morphology, was found equal to 0.722 for the synthesis without POA and 0.777 for the synthesis with POA, indicating that the nanoparticles were in both cases dense spheres (theoretically 0.775). Polydispersity index (I_p) of

Table I Gyration and Hydrodynamic Radii (R_g and R_h), Polydispersity Index (I_p) and Zeta Potential (ζ) of PVDF Nanoparticles Synthesized with or Without Surfactant (POA), PVDF-g-PAA, PVDF-g-PAA-mTEG and PVDF-g-PAA-mTEG-CBO-P11-CyTE777 Nanoparticles Determined by FESEM, SLS, SANS and/or DLS

	FESEM	SLS	SANS	DLS		
	R (nm)	R_g (nm)	R (nm)	R_h (nm)	I_p[c]	ζ (mV)
PVDF[a]	110 ± 5	86 ± 4	ND	102 ± 5	0.070 ± 0.008	−43.9 ± 0.3
PVDF[b]	55 ± 5	49 ± 3	61 ± 1	59 ± 4	0.002 ± 0.003	−42.7 ± 0.2
PVDF-g-PAA	58 ± 5	ND	63 ± 5	103 ± 5	0.228 ± 0.041	−57.3 ± 0.2
PVDF-g-PAA-mTEG	58 ± 5	ND	ND	103 ± 5	0.130 ± 0.024	−49.9 ± 0.7
PVDF-g-PAA-mTEG-CBO-P11-CyTE777	60 ± 5	ND	ND	135 ± 9	0.134 ± 0.031	−12.3 ± 4.6

[a] Synthesis without POA; [b] Synthesis with POA; [c] I_p given by Zetasizer (as I_p tends to 0, monodispersity is high); *ND* no determined

particles was calculated by DLS as a measurement of the distribution of size to appreciate the homogeneity of the sample. The very low I_p values indicated that PVDF nanoparticles were monodisperse for both syntheses. In addition, the zeta potential values found by DLS were around −40 mV and indicated stable dispersions in water. In theory, high zeta potential values, being positive or negative, tend to stabilize particle suspension. The electrostatic repulsion between particles with the same electric charge prevents the aggregation of the spheres (27). The negative values of zeta potential (presence or absence of POA) come from initiator sulfonate groups and polymer surface charges. Indeed, PVDF is a dielectric polymer, and electrons are trapped at its surface.

In Situ Radio-Grafting of Poly(Acrylic Acid) (PAA)

Introducing negatively charged hydrophilic groups onto hydrophobic PVDF polymer is necessary to confer biological hemocompatibility to nanoparticles. These functional groups could also be used for the anchoring of biological molecules by covalent binding (28). Acrylic acid (AA) was chosen as the monomer to obtain grafted PVDF-g-PAA polymer, as its radical polymerization is easy to control. Pending carboxylic acid functions could allow subsequent coupling. The lack of reactive functions in PVDF makes the functionalization difficult with usual chemical reactions. Thus, irradiation was used to create free radicals on the surface of the solid and initiate the polymerization of monomer leading to the formation of a grafted polymer. Radiation initiation is one of the cleanest grafting methods available, since molecular initiator or catalysts are not required. In a previous work, we reported the grafting of AA on PVDF nanoparticles after their irradiation (*post*-radio-grafting) (19). However, electron paramagnetic resonance and differential scanning calorimetry studies showed a relative instability of radicals initiated under irradiation in comparison with PVDF films, decreasing the radical amount available for *post*-polymerization of AA. In order to circumvent this problem, PVDF-g-PAA nanoparticles were directly prepared by irradiation of PVDF nanoparticle suspensions *in situ* in a monomer solution. Additionally, this *in situ* method allowed us to keep nanoparticles in suspension, preventing aggregation. Moreover, AA monomers act as radiation protectors and reduce the risk of degradation of the polymer substrate by the radiation itself (29).

In agreement with previous studies (19,30,31), the FTIR spectrum of PVDF-g-PAA (Fig. 1) shows a characteristic absorption band at 1,726 cm^{-1} attributed to the C=O stretching vibration of the carboxylic acid of PAA. The PVDF CH_2 stretching vibrations give absorption bands at

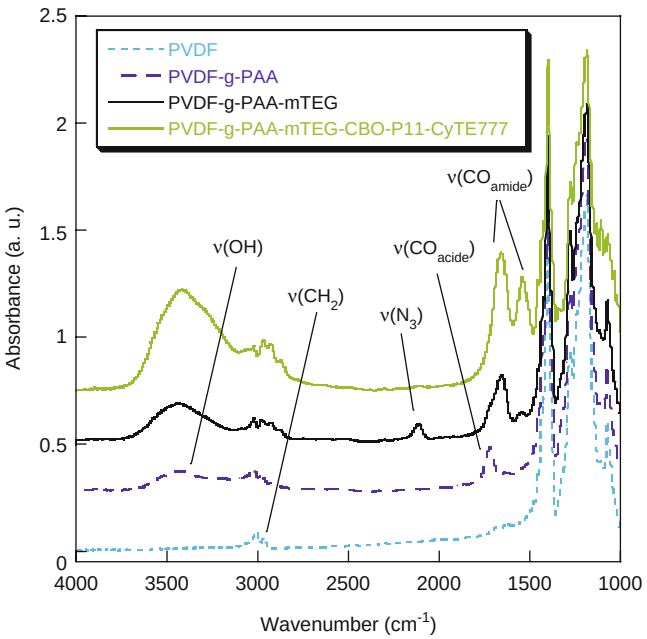

Fig. 1 FTIR transmission spectra of PVDF, PVDF-g-PAA, PVDF-g-PAA-mTEG and PVDF-g-PAA-mTEG-CBO-P11-CyTE777 nanoparticles. PVDF nanoparticles were irradiated at 5 kGy.

3,022 and 2,979 cm^{-1} which are superimposed with the OH vibrations of PAA band in the 2,500–3,500 cm^{-1} region. To estimate the grafting yields by FTIR, a calibration curve was performed by integration of the C=O stretching band from known amounts of a PAA standard in the KBr pellets (see Figure S1 in Electronic Supplementary Material). The yields of PAA grafting increase gradually with irradiation dose in agreement with the evolution of radical concentration (data not shown). Overall grafting yields are low (<7% w/w), and we assume that grafting occurred mainly onto the nanoparticles surface and not in the nanoparticles bulk. Indeed, radiation grafting to polymeric nanoparticles proceeds from the substrate surface, and as the nanoparticles swell, it progressively enters into substrate bulk. This mechanism known as the grafting front mechanism was first described in Chapiro's pioneer work in the early 1960s (32). To check this hypothesis, PVDF-g-PAA nanoparticles were analyzed by a surface technique named X-ray photoelectron spectroscopy (XPS) (see Figure S2 in Electronic Supplementary Material). First, survey spectra confirmed the PAA grafting with the presence of O_{1S} ray at 533 eV. Furthermore, ratios of deconvoluted C_{1S} peaks allowed a grafting yield estimation of 11 mol% over the 8 nm probed thickness. As the grafting yield of the whole nanoparticles was found equal to 2 mol% by FTIR, it consequently suggests an enrichment of PAA at the surface of nanoparticles.

The influence of PAA grafting on the nanoparticles dispersion was investigated by SANS. Scattering intensity per unit volume and total concentration unit of both PVDF and PVDF-g-PAA nanoparticles at different irradiation doses are shown in Fig. 2 (data treatment are shown in Electronic Supplementary Material). At high q, the shape of the spectra was similar, indicating that radiografting did not induce any significant change of the size and shape of nanoparticles. They remained spherical after irradiation in spite of the presence of PAA. Indeed, the grafting yields being low, they have a negligible effect on the nanoparticles morphology. On the opposite at low q, the scattered intensity decreased with the irradiation dose. An increase in repulsive interactions due to the charges of the increasing number of dissociated carboxylic functions is clearly indicated. These repulsive interactions were coroborated by higher negative zeta potential relative to PVDF nanoparticles (Table I), which favours colloidal stability, a very important property for a long blood circulation time.

Coupling of Spacer Arm (mTEG)

To increase the hydrophilicity of the polymer, to allow the coupling of the targeting peptide and improve its accessibility in the future biological environment, a spacer arm was coupled to carboxylic acid functions of PVDF-g-PAA nanoparticles. As a model, a short ethylene glycol was first chosen as spacer. A modified tetraethylene glycol (noted mTEG) with an amine function at one end and an azide function at the other end was prepared (24). The amine function was coupled to the carboxylic acid functions of PAA *via* an amide bond, using a water-soluble carbodiimide (EDC) as coupling agent (Scheme 1). FTIR spectrum of PVDF-g-PAA-mTEG nanoparticles (Fig. 1) shows specific amide bond absorptions (1,643 and 1,572 cm^{-1}), NH amide (3,700–3,130 cm^{-1}), CH_2 ether (2,950–2,840 cm^{-1}), azide stretching vibrations (2,112 cm^{-1}) and decrease of the COOH absorption band, in agreement with the covalent coupling of the amino spacer arm. Furthermore, when PVDF-g-PAA-mTEG nanoparticles were analyzed by XPS (see Figure S3 in Electronic Supplementary Material), a new peak corresponding to N_{1S} of azide and/or amide functions was observed, and the deconvoluted C_{1S} ray signal showed the contribution of both ether and amide functions. These results confirm that the spacer arm was grafted to nanoparticles and not simply adsorbed. The coupling of spacer arm did not modify the size of nanoparticles as shown by FESEM and DLS data in Table I. Furthermore, zeta potential was maintained negative and confers a high stability to the nanoparticle suspensions.

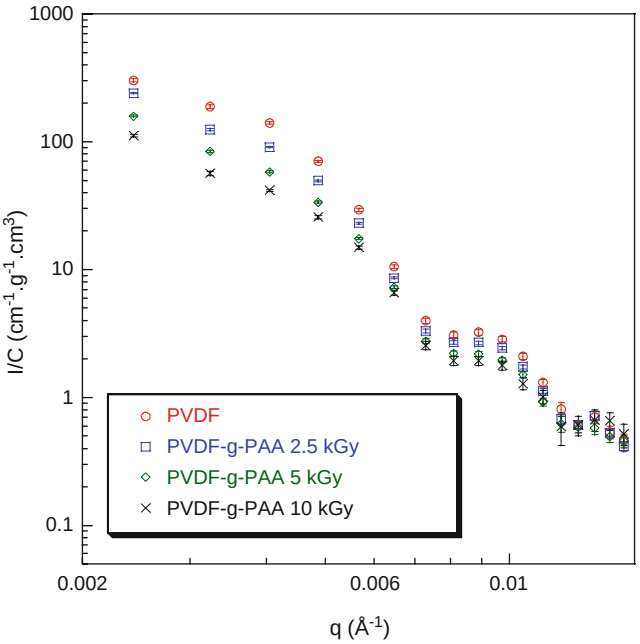

Fig. 2 SANS spectra of PVDF nanoparticles before irradiation and PVDF-g-PAA nanoparticles at different irradiation doses. The spectra were normalized to the concentration of nanoparticles in D_2O.

Synthesis of Fluorescent Alkyne-modified Peptide and "Click" Coupling on Azido Nanoparticles

CBO-P11, a 17-amino acid cyclo-peptide encompassing residues 79–93 of VEGF, was synthesized as previously

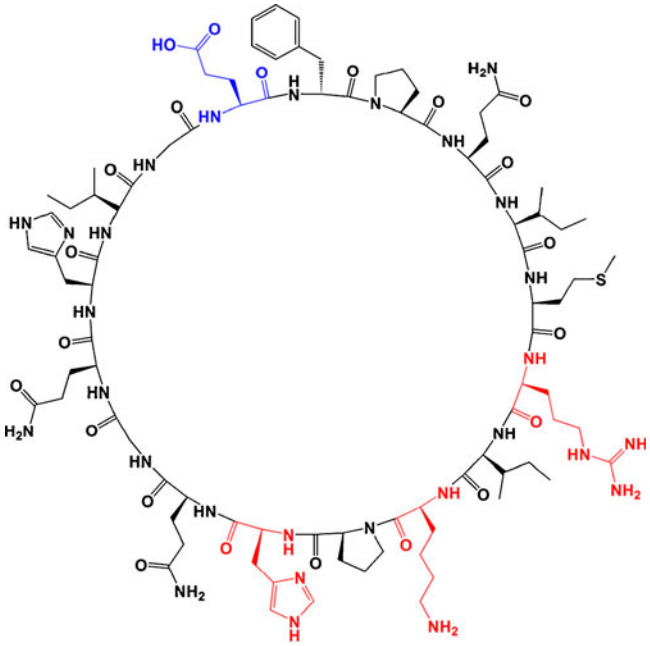

Fig. 3 Chemical structure of CBO-P11. The three basic amino acids essential for the interaction with VEGF receptors are in red. Amino acid which allowed the peptide functionalization is in blue.

described (Fig. 3) (11). CBO-P11 was shown to bind to VEGFR-2 and inhibit VEGF binding with a half-maximal inhibitory concentration (IC_{50}) of 1.3 μM. This high affinity makes CBO-P11 a suitable candidate for targeted anti-angiogenic therapy.

The anchoring of CBO-P11 on polymeric nanoparticles required a method allowing to keep the integrity of essential basic amino-acids. The copper(I)-catalyzed Huisgen 1,3-dipolar cycloaddition, named "click" chemistry, has proven to be an easy path to covalently couple azides and acetylenes (33–35). To apply this reaction on the azido nanoparticles, CBO-P11 has been modified with a pendant alkyne moiety. This acetylene was introduced between a fluorescent cyanine dye (CyTE777) (25) and CBO-P11 using lysine as intermediate. The peptide was labelled with a cyanine to detect and locate nanoparticles. Cyanines belong to the family of near infrared (NIR) probes with emissions above 700 nm. The use of NIR dyes shows relevant advantages, such as minimal interfering absorption, inexpensive laser diode excitation, reduced scattering and enhanced tissue penetration depth (36). Thus, Fmoc-Lys(Boc)-OH was modified with an alkyne function from propargylamine *via* EDC-mediated amide coupling. Then, after a consecutive protecting group removal and amide coupling, we obtained CyTE777-Lys(CBO-P11)-propargyl amide (Scheme 2).

Then, the fluorescent alkyne-modified peptide [5] was conjugated to azido-functionalized PVDF-g-PAA-mTEG nanoparticles in a H_2O/*t*-BuOH solvent system (Scheme 1). The opportunity to perform "click" reaction in aqueous media allowed us to keep nanoparticles in their mother solution and limit the risk of aggregation. Additionally, it avoids the use of toxic solvents, which is crucial for biological applications. After reaction and purification, the fluorescent peptide content was estimated by UV spectroscopy and found equal to 4.3 mol%. FTIR spectra show a decrease of azide band at 2,112 cm^{-1} and an increase of amide bands after reaction (Fig. 1), in agreement with a covalent coupling. Fluorescence spectra (Fig. 4A) show an absorption maximum λ_{exc}=785 nm and an emission maximum λ_{em}=843 nm for PVDF-g-PAA-mTEG-CBO-P11-CyTE777 nanoparticles.

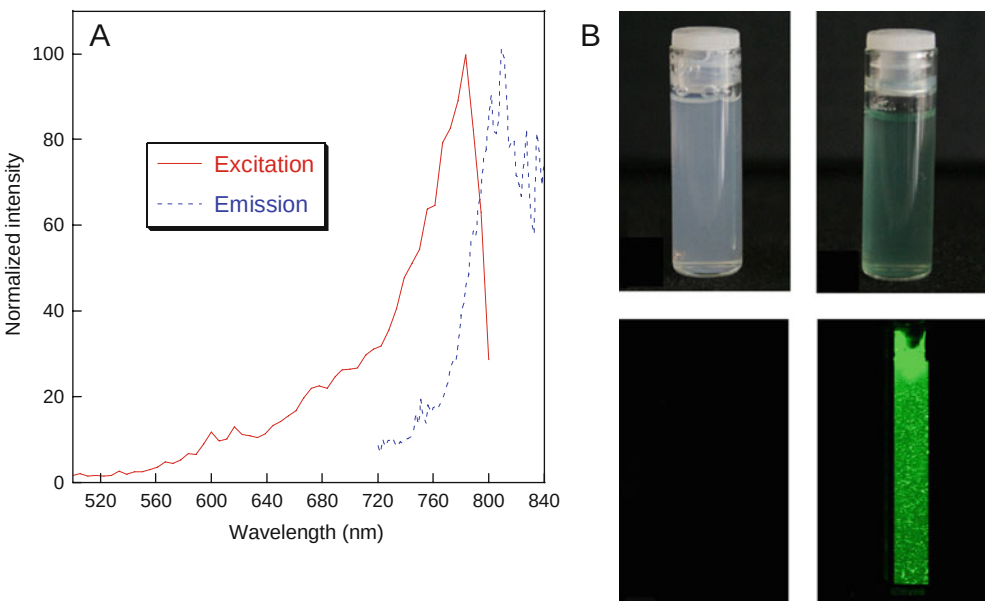

Fig. 4 (**A**) Normalized excitation and emission spectra of 2.0 μM aqueous solutions of PVDF-g-PAA-mTEG-CBO-P11-CyTE777 nanoparticles. (**B**) Visible images of PVDF nanoparticles (*left top*) and PVDF-g-PAA-mTEG-CBO-P11-CyTE777 nanoparticles (*right bottom*). Fluorescence images of PVDF nanoparticles (*left top*) and PVDF-g-PAA-mTEG-CBO-P11-CyT777 nanoparticles (*right bottom*) recorded in water (1.7 g/ml, i.e. 60 μM of CyTE777) by Odyssey at 800 nm.

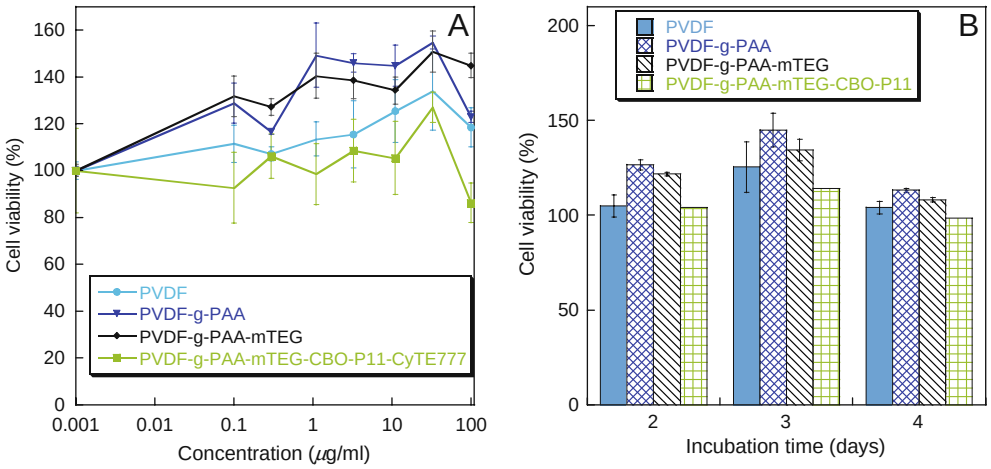

Fig. 5 Cytotoxicity profiles for HCMEC. (**A**) Effect of the nanoparticles on cell viability after a three-day incubation with either PVDF, PVDF-g-PAA, PVDF-g-PAA-mTEG or PVDF-g-PAA-mTEG-CBO-P11-CyTE777. (**B**) Cell viability in time after incubation with 11 μg/ml of nanoparticles.

To demonstrate the potential use of these devices for imaging, fluorescence images of PVDF and PVDF-g-PAA-mTEG-CBO-P11-CyTE777 nanoparticles in water suspension were recorded using a fluorescence scanner (Odyssey) commonly available in biological laboratories (Fig. 4B). The image for labelled nanoparticles (PVDF-g-PAA-mTEG-CBO-P11-CyTE777) shows very bright green color, whereas the image remains dark when nanoparticles are not labelled with fluorescent probe. Nanoparticles did not quench the fluorescence of cyanine after conjugation. The high fluorescence intensity suggests a great potential for an application in medical imaging.

Cytotoxicity Assays

To assess the biocompatibility of functionalized nanoparticles, human brain endothelial cells (HCMEC) were exposed to nanoparticles at different concentrations for 2, 3 or 4 days. Cell viability was then checked by measuring the absorbance of WST-1 reagent on an ELISA plate reader (Fig. 5). WST-1, a modified tetrazolium salt, is reduced to water-soluble formazan in the mitochondria of living cells. This reduction only takes place when mitochondrial reductase enzymes are active, and therefore conversion can be directly related to cell viability (37). Data revealed the absence of toxicity of the nanoparticles, whatever the concentration used, after four days of incubation. Unexpectedly, we observed an increase in WST-1 signal under high concentrations of nanoparticles, suggesting a slight metabolic effect of these compounds on cells. Similar results were obtained using other endothelial cell types from different tissue and animal origins, including porcine aortic endothelial (PAE) cells, and human umbilical vein endothelial cells (HUVEC) (not shown). From these results, functionalized PVDF nanoparticles thus appeared to be biocompatible.

Cell Uptake Assays

In order to check that CBO-P11 kept its binding affinity for VEGF receptors after conjugation on nanoparticles, cell uptake assays were performed on PAE cells which were

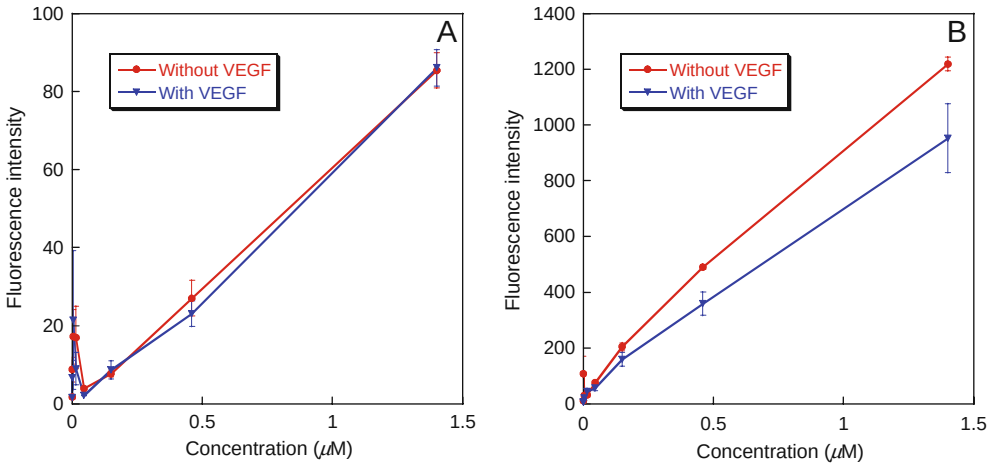

Fig. 6 Fluorescence intensity in PAE cells incubated with (**A**) PVDF-g-PAA-mTEG-CyTE777 nanoparticles and (**B**) PVDF-g-PAA-mTEG-CBO-P11-CyTE777 nanoparticles, with or without 100 ng/ml VEGF.

modified to overexpress VEGFR-2. PAE cells were incubated with fluorescent nanoparticles containing CBO-P11 (PVDF-g-PAA-mTEG-CBO-P11-CyTE777) or with control fluorescent nanoparticles without peptide (PVDF-g-PAA-mTEG-CyTE777). Control cells were also incubated in the presence of an excess (100 ng/ml) of VEGF to block receptors, thus preventing VEGFR-2-mediated uptake of nanoparticles. Fluorescence was quantified at different fluorophore concentrations (Fig. 6). Figure 6A showed a similar uptake profile with or without VEGF for PVDF-g-PAA-mTEG-CyTE777 nanoparticles. In contrast, fluorescence intensity for PVDF-g-PAA-mTEG-**CBO-P11**-CyTE777 nanoparticles was significantly higher (22%) in the absence of VEGF relative to cells incubated with VEGF (Fig. 6B). This indicates that VEGF receptors on the cells were partially responsible for the nanoparticles uptake, suggesting a specific interaction between CBO-P11 and VEGF receptors. Therefore, the anchoring of the VEGF receptor-targeting peptide on the surface of nanoparticles did not impede its binding to VEGF receptors. This indicates that nanoparticles containing CBO-P11 may represent useful vectors for targeting tumor angiogenesis.

CONCLUSION

In this paper, we have developed novel polymeric nanoparticles as a tool for targeting tumor angiogenesis. CBO-P11, a VEGFR-2-specific cylco-peptide, was successfully conjugated on the surface of PVDF nanoparticles using "click" chemistry. The nanoparticles were prepared from monomer of PVDF by radical aqueous emulsion polymerization. They were functionalized by *in situ* radiation grafting of acrylic acid in aqueous solution. This process was chosen to prevent aggregation and optimize the radical polymerization initiation step. Then, a spacer with azide function was coupled to nanoparticles to increase the hydrophilicity of the polymer. In the future, a longer poly (ethylene glycol) spacer will have to be considered to provide a better colloidal stability and to avoid immune system identification (mode "stealth"). CBO-P11 was labelled with an NIR cyanine dye bearing an alkyne function which allowed "click" reaction with azide functions on the periphery of nanoparticles. From SANS, FESEM, SLS and DLS, nanoparticles appeared spherical, dense and monodisperse. SANS data indicated a relative stable dispersion due to electrostatic interactions of PAA grafted onto PVDF nanoparticles. This stability of the nanoparticles should favour a long blood circulation time. IRTF and XPS studies confirmed a grafting on the surface of nanoparticles, making the reactive functions more available. Furthermore, every synthesis step was run in aqueous solution, leaving nanoparticles in a favourable environment for medical application. Cytotoxicity assays revealed the absence of toxicity after incubation of nanoparticles on HCMEC, suggesting the biocompatibility of theses nanodevices. Cell uptake assays showed that nanoparticle-conjugated CBO-P11 retained its binding specificity for VEGFR-2. These results are very encouraging to use these novel nanodevices for targeting tumor vasculature. In addition, the labelling with a cyanine dye may be useful for *in vivo* optical imaging due to the high depth of NIR probes. "Click" chemistry is highly selective and can be broadly applicable to a panel of molecules (therapeutic drugs, imaging agents etc.). As a matter of fact, a combination of these labelled nanoparticles with therapeutic agents to obtain multifunctional system for drug delivery is under study.

ACKNOWLEDGMENTS

We are grateful to François Bauer (Piezotech SA) for the PVDF nanoparticles synthesis. We also thank Dr. Christophe Schatz (Laboratoire de Chimie des Polymères Organiques, UMR CNRS 5629, University of Bordeaux, France) for dynamic light scattering experiments and La Ligue Contre le Cancer for its financial support.

REFERENCES

1. Brigger I, Dubernet C, Couvreur P. Nanoparticles in cancer therapy and diagnosis. Adv Drug Deliv Rev. 2002;54(5):631–51.
2. Matsumura Y, Maeda H. A new concept for macromolecular therapeutics in cancer chemotherapy: mechanism of tumoritropic accumulation of proteins and the antitumor agent Smancs. Cancer Res. 1986;46(12 Part 1):6387–92.
3. Ruoslahti E. Targeting tumor vasculature with homing peptides from phage display. Semin Cancer Biol. 2000;10(6):435–42.
4. Folkman J. Tumor angiogenesis: therapeutic implications. N Engl J Med. 1971;285:1182–6.
5. de Vries C, Escobedo JA, Ueno H, Houck K, Ferrara N, Williams LT. The *fms*-like tyrosine kinase, a receptor for vascular endothelial growth factor. Science. 1992;255(5047):989–91.
6. Terman BI, Dougher-Vermazen M, Carrion ME, Dimitrov D, Armellino DC, Gospodarowicz D, *et al.* Identification of the KDR tyrosine kinase as a receptor for vascular endothelial cell growth factor. Biochem Biophys Res Commun. 1992;187(3):1579–86.
7. Ferrara N, Hillan KJ, Novotny W. Bevacizumab (Avastin), a humanized anti-VEGF monoclonal antibody for cancer therapy. Biochem Biophys Res Commun. 2005;333(2):328–35.
8. Ferrara N. Role of vascular endothelial growth factor in physiologic and pathologic angiogenesis: therapeutic implications. Semin Oncol. 2002;29(6, Supplement 16):10–4.
9. Ferrara N, Davis-Smyth T. The biology of vascular endothelial growth factor. Endocr Rev. 1997;18(1):4–25.
10. Eichhorn ME, Strieth S, Dellian M. Anti-vascular tumor therapy: recent advances, pitfalls and clinical perspectives. Drug Resist Updat. 2004;7(2):125–38.
11. Zilberberg L, Shinkaruk S, Lequin O, Rousseau B, Hagedorn M, Costa F, *et al.* Structure and inhibitory effects on angiogenesis and tumor development of a new vascular endothelial growth inhibitor. J Biol Chem. 2003;278(37):35564–73.

12. Braga FJC, Rogero SO, Couto AA, Marques RFC, Ribeiro AA, Campos JSdC. Characterization of PVDF/HAP composites for medical applications. Mater Res. 2007;10:247–51.
13. Ding N, Pacetti SD, Tang F-W, Gada M, Roorda W. XIENCE V™ stent design and rationale. J Interv Cardiol. 2009;22:S18–27.
14. Klinge U, Klosterhalfen B, Ottinger AP, Junge K, Schumpelick V. PVDF as a new polymer for the construction of surgical meshes. Biomaterials. 2002;23(16):3487–93. doi:10.1016/S0142-9612(02)00070-4.
15. Conze J, Junge K, Weiß C, Anurov M, Oettinger A, Klinge U, *et al.* New polymer for intra-abdominal meshes—PVDF copolymer. J Biomed Mater Res B Appl Biomater. 2008;87B(2):321–8.
16. Berger D. Prevention of parastomal hernias by prophylactic use of a specially designed intraperitoneal onlay mesh (Dynamesh IPST®). Hernia. 2008;12(3):243–6.
17. Klee D, Ademovic Z, Bosserhoff A, Hoecker H, Maziolis G, Erli H-J. Surface modification of poly(vinylidenefluoride) to improve the osteoblast adhesion. Biomaterials. 2003;24(21):3663–70. doi:10.1016/S0142-9612(03)00235-7.
18. Valentini RF, Vargo TG, Gardella Jr JA, Aebischer P. Electrically charged polymeric substrates enhance nerve fibre outgrowth *In vitro*. Biomaterials. 1992;13(3):183–90. doi:10.1016/0142-9612(92)90069-Z.
19. Deshayes S, Maurizot V, Clochard M-C, Berthelot T, Baudin C, Déléris G. Synthesis of specific nanoparticles for targeting tumor angiogenesis using electron-beam irradiation. Radiat Phys Chem. 2010;79(3):208–13.
20. von Maltzahn G, Ren Y, Park J-H, Min D-H, Kotamraju VR, Jayakumar J, *et al.* Tumor cell targeting with "click" nanoparticles. Bioconjug Chem. 2008;19(8):1570–8.
21. Opsteen JA, Brinkhuis RP, Teeuwen RLM, Lowik DWPM, Hest JCMV. "Clickable" polymersomes. Chem Commun. 2007;30:3136–8.
22. Nicolas J, Bensaid F, Desmaele D, Grogna M, Detrembleur C, Andrieux K, *et al.* Synthesis of highly functionalized poly(alkyl cyanoacrylate) nanoparticles by means of click chemistry. Macromolecules. 2008;41(22):8418–28.
23. Weksler BB, Subileau EA, Perriere N, Charneau P, Holloway K, Leveque M, *et al.* Blood-brain barrier-specific properties of a human adult brain endothelial cell line. FASEB J. 2005;19(13):1872–4.
24. Gonçalves M, Estieu-Gionnet K, Berthelot T, Laïn G, Bayle M, Canron X, *et al.* Design, synthesis, and evaluation of original carriers for targeting vascular endothelial growth factor receptor interactions. Pharm Res. 2005;22(8):1411–21. doi:10.1007/s11095-005-5265-9.
25. Hilderbrand SA, Kelly KA, Weissleder R, Tung C-H. Monofunctional near-infrared fluorochromes for imaging applications. Bioconjug Chem. 2005;16(5):1275–81.
26. Moody CA, Field JA. Perfluorinated surfactants and the environmental implications of their use in fire-fighting foams. Environ Sci Technol. 2000;34(18):3864–70.
27. Chansiri G, Lyons RT, Patel MV, Hem SL. Effect of surface charge on the stability of oil/water emulsions during steam sterilization. J Pharm Sci. 1999;88(4):454–8.
28. Steffens GCM, Nothdurft L, Buse G, Thissen H, Höcker H, Klee D. High density binding of proteins and peptides to poly(D, L-lactide) grafted with polyacrylic acid. Biomaterials. 2002;23(16):3523–31.
29. Stannett V. Grafting. Radiat Phys Chem. 1981;18(1–2):215–22.
30. Betz N, Begue J, Gonçalves M, Gionnet K, Déléris G, Le Moël A. Functionalisation of PAA radiation grafted PVDF. Nucl Instrum Methods Phys Res Sect B. 2003;208:434–41.
31. Clochard MC, Begue J, Lafon A, Caldemaison D, Bittencourt C, Pireaux JJ, *et al.* Tailorring bulk and surface grafting of poly(acrylic acid) in electron-irradiated PVDF. Polymer. 2004;45(26):8683–94.
32. Chapiro A. In: Gaylord NG, Adler G, editors. Radiation chemistry of polymeric systems high polymers. New York: Interscience; 1962.
33. Rostovtsev V, Green L, Fokin V, Sharpless K. A stepwise Huisgen cycloaddition process: copper(I)-catalyzed regioselective "ligation" of azides and terminal alkynes. Angew Chem Int Ed. 2002;41(14):2596–9.
34. Perez-Balderas F, Ortega-Munoz M, Morales-Sanfrutos J, Hernandez-Mateo F, Calvo-Flores FG, Calvo-Asin JA, *et al.* Multivalent neoglycoconjugates by regiospecific cycloaddition of alkynes and azides using organic-soluble copper catalysts. Org Lett. 2003;5(11):1951–4.
35. Hiki S, Kataoka K. A facile synthesis of azido-terminated heterobifunctional poly(ethylene glycol)s for "click" conjugation. Bioconjug Chem. 2007;18(6):2191–6.
36. Rao J, Dragulescu-Andrasi A, Yao H. Fluorescence imaging *in vivo*: recent advances. Curr Opin Biotechnol. 2007;18:17–25.
37. Berridge MV, Tan AS, McCoy KD, Wang R. The biochemical and cellular basis of cell proliferation assays that use tetrazolium salts. Biochemica. 1996;4:15–20.